We are IntechOpen, the world's leading publisher of Open Access books Built by scientists, for scientists

4,800
Open access books available

122,000
International authors and editors

135M
Downloads

Our authors are among the

154
Countries delivered to

TOP 1%
most cited scientists

12.2%
Contributors from top 500 universities

CLARIVATE ANALYTICS BOOK CITATION INDEX INDEXED

WEB OF SCIENCE™

Selection of our books indexed in the Book Citation Index in Web of Science™ Core Collection (BKCI)

Interested in publishing with us?
Contact book.department@intechopen.com

Numbers displayed above are based on latest data collected.
For more information visit www.intechopen.com

21

Non-Linear Periodic and Quasi-Periodic Vibrations in Mechanical Systems - On the use of the Harmonic Balance Methods

Emmanuelle Sarrouy and Jean-Jacques Sinou
Laboratoire de Tribologie et Dynamique des Systèmes UMR-CNRS 5513
Ecole Centrale de Lyon, 36 avenue Guy de Collongue 69134 Ecully Cedex
France

1. Introduction

Due to the fact that non-linear dynamical structures are encountered in many areas of science and engineering, strong developments in the treatment of non-linear differential equations have been proposed and various computational techniques are commonly applied in a wide range of mechanical engineering problems.

The most common techniques for predicting the non-linear behaviour of systems are based on numerical integration over time. However, the use of these methods for non-linear systems with many degrees of freedom can be rather expensive and requires considerable resources both in terms of computation time and data storage. Due to the complexity of non-linear systems and to save time, approximate methods for the study of non-linear oscillating systems described by ordinary non-linear differential equations are usually required. In this category, the most popular methods for approximating the stationary non-linear responses of systems are the harmonic balance methods. The principal idea for these non-linear methods is to replace the non-linear responses and the non-linear forces in the dynamical systems by constructing linear functions such as Fourier series. The main objective of these non-linear methods is to extract and characterize the non-linear behaviours of mechanical systems by using non-linear approximations.

In this chapter, the general formulation and extensions of the harmonic balance method will be presented. The chapter is divided into four parts. Firstly we propose to present the general formulation and the basic concept of the harmonic balance method to find periodic oscillations of non-linear systems. Secondly a generalization of the method is exposed to treat quasi-periodic solutions. Thirdly, a condensation procedure that keeps only the non-linear degrees of freedom of the mechanical system is described. This technique may be of great interest to reduce the original non-linear system and to calculate the dynamical behaviour of non-linear systems with many degrees of freedom. The last part presents the classical continuation procedures that let us follow the evolution of a solution as a system parameter varies. For these two steps procedures, several prediction methods (secant, tangent and

Lagrange polynomial methods) and correction methods (arc length, pseudo arc length and Moore-Penrose methods) are detailed.

2. General theory of the harmonic balance method

The most general formulation for a non-linear dynamical system is

$$\underline{\underline{M}}\,\underline{\ddot{q}} + \underline{\underline{C}}\,\underline{\dot{q}} + \underline{\underline{K}}\,\underline{q} + \underline{\hat{f}}(t, \underline{q}, \underline{\dot{q}}) = \underline{f_e}(t) \tag{1}$$

where $\underline{\underline{M}}$, $\underline{\underline{C}}$ and $\underline{\underline{K}}$ are respectively the mass, damping (including gyroscopic effects if any) and stiffness matrices, $\underline{\hat{f}}(t, \underline{q}, \underline{\dot{q}})$ stands for the non-linear effects in the system and $\underline{f_e}(t)$ the external forces. $\underline{q}$ is the displacement vector with size n. Looking for periodic solutions $\underline{q}(t)$ with a determined period T, it is legitimate to look for the signal as a Fourier series which is truncated for the sake of the numerical application. Thus we assume that the non-linear dynamical response of the system may be approximated by finite Fourier series with $\omega = \frac{2\pi}{T}$ the fundamental pulsation:

$$\underline{q}(t) = \frac{\underline{a}_0}{\sqrt{2}} + \sum_{k=1}^{m} \left(\underline{a}_k \cos(k\omega t) + \underline{b}_k \sin(k\omega t)\right) \tag{2}$$

where m is the order of the Fourier series. $\underline{a}_0$, $\underline{a}_k$ and $\underline{b}_k$ define the unknown coefficients of the finite Fourier series. It should be noted that these coefficients define $\underline{\dot{q}}$ and $\underline{\ddot{q}}$ too.
The number of harmonic coefficients is selected on the basis of the number of significant harmonics expected in the non-linear dynamical response. Generally speaking, harmonic components become less significant when m increases. This formulation includes only harmonic and super-harmonic responses of the system. Some terms can be added to take sub-harmonics (with pulsation $\frac{k'}{l}\omega$) into account. So as to keep simple equations these terms will not be included in the following sections.
In order to determine the value of the $n \times (2m+1)$ unknowns, the decomposition (2) is reinjected in (1); the time variable is then removed by projecting the resulting system onto the basis $(1/\sqrt{2}, \cos(k\omega t), \sin(k\omega t))_{(k=1,..,m)}$ using the scalar product:

$$< f, g >_T = \frac{2}{T} \int_0^T f(t) g(t) dt \tag{3}$$

This leads to a set of $n \times (2m+1)$ non-linear (non-differential) equations that can be solved using a dedicated algorithm such as Broyden method (Broyden, 1965):

$$\underline{H}(\underline{\tilde{x}}) = \underline{\underline{H_l}}\,\underline{\tilde{x}} + \underline{\hat{H}}(\underline{\tilde{x}}) - \underline{H_e} = \underline{0} \tag{4}$$

where $\underline{\tilde{x}}$ regroups the unknowns $\underline{a}_0$, $\underline{a}_k$ and $\underline{b}_k$,

$$\underline{\tilde{x}} = \left\{ \begin{array}{ccccccc} \underline{a}_0^T & \underline{a}_1^T & \underline{b}_1^T & \dots & \underline{a}_m^T & \underline{b}_m^T \end{array} \right\}^T, \tag{5}$$

$\underline{\underline{H_l}}$ contains the contribution of the linear part of (1), $\underline{\hat{H}}(\underline{\tilde{x}})$ is the projection of the non-linear part and $\underline{H_e}$ the one of the external forces. For further use, the following quantities are

defined: first, the blocks of the $\underline{\underline{H_l}}$ (block diagonal) matrix

$$\underline{\underline{H_l}} = \begin{bmatrix} \underline{\underline{\Lambda_0}} & \underline{\underline{0}} & \cdots & \\ \underline{\underline{0}} & \underline{\underline{\Lambda_1}} & \underline{\underline{0}} & \cdots \\ \cdots & \underline{\underline{0}} & \underline{\underline{\Lambda_k}} & \underline{\underline{0}} \\ & \cdots & \underline{\underline{0}} & \underline{\underline{\Lambda_m}} \end{bmatrix}, \tag{6a}$$

$$\underline{\underline{\Lambda_0}} = \underline{\underline{K}} \in \mathcal{M}_n(\mathbb{R}) \tag{6b}$$

$$\forall\, k \in \{1, \ldots, m\},\ \underline{\underline{\Lambda_k}} = \begin{bmatrix} \underline{\underline{K}} - (k\omega)^2 \underline{\underline{M}} & (k\omega)\underline{\underline{C}} \\ -(k\omega)\underline{\underline{C}} & \underline{\underline{K}} - (k\omega)^2 \underline{\underline{M}} \end{bmatrix} \in \mathcal{M}_{2n}(\mathbb{R}) \tag{6c}$$

Then, the approximation of the non-linear contribution using its projections $\underline{c_0}$, $\underline{c_k}$ and $\underline{d_k}$ onto $1/\sqrt{2}$, $\cos(k\omega t)$ and $\sin(k\omega t)$ respectively is written as follow:

$$\underline{\hat{f}}(t, \underline{q}, \underline{\dot{q}}) \approx \frac{\underline{c_0}}{\sqrt{2}} + \sum_{k=1}^{m} \left(\underline{c_k} \cos(k\omega t) + \underline{d_k} \sin(k\omega t) \right) \tag{7}$$

Using this notations, $\underline{\hat{H}}(\underline{\tilde{x}})$ is the vector

$$\underline{\hat{H}}(\underline{\tilde{x}}) = \left\{ \begin{array}{ccccccc} \underline{c_0}^T & \underline{c_1}^T & \underline{d_1}^T & \cdots & \underline{c_m}^T & \underline{d_m}^T \end{array} \right\}^T \tag{8}$$

Cameron and Griffin (Cameron & Griffin, 1989) suggested to compute these quantities using an alternate frequency/time domain (AFT) method. First, an Inverse Fast Fourier Transform (IFFT) is used to recompose $\underline{q}(t_j)$ and $\underline{\dot{q}}(t_j)$ from $\underline{a_0}$, $\underline{a_k}$, $\underline{b_k}$ coefficients for some $t_j \in [0, T]$. Then, for each time step t_j the $\underline{\hat{f}}(t_j, \underline{q}(t_j), \underline{\dot{q}}(t_j))$ vectors are computed and $\underline{c_0}$, $\underline{c_k}$ and $\underline{d_k}$ projections are finally obtained using a Fast Fourier Transform (FFT) to switch back into the frequency space.
Usually, the external forces are T-periodic and there is no numerical computation required to obtain the $\underline{H_e}$ vector.

3. Extension of the Harmonic Balance Method for multiple excitations

Now, the general case in which the structural system is excited by several incommensurable frequencies $\omega_1, \omega_2, \ldots, \omega_p$ is discussed. The previous non-linear dynamical equation (1) is considered with multiple excitations contained in the external excitation forces $\underline{f_e}(t)$. So, non-linear responses are no longer periodic when oscillatory systems are subjected to p incommensurable frequencies. The non-linear oscillations contain the frequency components of any linear combination of the incommensurable frequency components

$$k_1\omega_1 + k_2\omega_2 + \cdots + k_j\omega_j + \cdots + k_p\omega_p \quad \text{with} \quad k_j = -m, -m+1, \ldots, -1, 0, 1, \ldots, m-1, m \tag{9}$$

where m defines the order for each fundamental frequency and p the number of incommensurable frequencies.

Thus the approximation of the dynamic non-linear response of equation (1) can be expressed with a generalized Fourier series in the following form

$$\underline{q}(t) = \sum_{k_1=-m}^{m} \sum_{k_2=-m}^{m} \cdots \sum_{k_p=-m}^{m} \left(\underline{a}_{k_1,k_2,\ldots,k_p} \cos\left(\sum_{j=1}^{p} k_j \omega_j t \right) \underline{b}_{k_1,k_2,\ldots,k_p} \sin\left(\sum_{j=1}^{p} k_j \omega_j t \right) \right) \quad (10)$$

where $\underline{a}_{k_1,k_2,\ldots,k_p}$ and $\underline{b}_{k_1,k_2,\ldots,k_p}$ define the unknown Fourier coefficients of any linear combinations of the incommensurable frequency components $\omega_1, \omega_2, \ldots, \omega_p$. For the reader comprehension, it may be noted that a definition for retaining m harmonics in a multiple Fourier series can be given by (Kim & Choi, 1997)

$$\sum_{j=1}^{p} |k_j| \leq m \quad (11)$$

Considering that all harmonics at negative combination frequencies can be replaced by harmonic terms at positive combination frequencies due to the following trigonometric relation

$$\cos\left(\sum_{j=1}^{p} k_j \omega_j t \right) = \cos\left(\sum_{j=1}^{p} -k_j \omega_j t \right) \quad (12)$$

$$\sin\left(\sum_{j=1}^{p} k_j \omega_j t \right) = -\sin\left(\sum_{j=1}^{p} -k_j \omega_j t \right) \quad (13)$$

it may be concluded that only terms at positive combination frequencies (i.e. $\sum_{j=1}^{p} k_j \omega_j t \geq 0$) can be retained in the non-linear response and non-linear force expressions.
So, the previous expression (10) can be rewritten in a condensed form

$$\underline{q}(t) = \frac{\underline{a}_0}{\sqrt{2}} + \sum_{\underline{k} \in \mathbb{Z}^p} \underline{a}_{\underline{k}} \cos\left(\underline{k}.\underline{\omega}\right) t + \sum_{\underline{k} \in \mathbb{Z}^p} \underline{b}_{\underline{k}} \sin\left(\underline{k}.\underline{\omega}\right) t \quad (14)$$

where the $(.)$ denotes the dot product, $\underline{k}$ is the harmonic number vector of each frequency direction and $\underline{\omega}$ is the vector of the p incommensurable frequencies considered in the solution. The contributions $\underline{a}_{\underline{k}}$ and $\underline{b}_{\underline{k}}$ contain the new Fourier decomposition of cosine and sine terms corresponding to the positive frequency combinations.
For convenience, it is wise to deal with a multiple time parameter. By introducing a non dimensional multiple time parameter $\underline{\tau} = \underline{\omega} t$ that refers to hyper-time concept proposed by (Kim & Choi, 1997), the approximated non-linear expression (14) is composed from elements of cosine and sine terms such as

$$\underline{q}(\underline{\tau}) = \frac{\underline{a}_0}{\sqrt{2}} + \sum_{\underline{k} \in \mathbb{Z}^p} \underline{a}_{\underline{k}} \cos\left(\underline{k}.\underline{\tau}\right) + \sum_{\underline{k} \in \mathbb{Z}^p} \underline{b}_{\underline{k}} \sin\left(\underline{k}.\underline{\tau}\right) \quad (15)$$

Injecting this in Eq. (1), one gets

$$\underline{\underline{K}}\frac{\underline{a}_0}{\sqrt{2}} + \sum_{\underline{k}\in\mathbb{Z}^p}\left(\left(\underline{\underline{K}} - (\underline{k}.\underline{\omega})^2\,\underline{\underline{M}}\right)\underline{a}_{\underline{k}} + \left((\underline{k}.\underline{\omega})\,\underline{\underline{C}}\right)\underline{b}_{\underline{k}}\right)\cos\left(\underline{k}.\underline{\tau}\right) + \sum_{\underline{k}\in\mathbb{Z}^p}\left(\left(\underline{\underline{K}} - (\underline{k}.\underline{\omega})^2\,\underline{\underline{M}}\right)\underline{b}_{\underline{k}} - \left((\underline{k}.\underline{\omega})\,\underline{\underline{C}}\right)\underline{a}_{\underline{k}}\right)\sin\left(\underline{k}.\underline{\tau}\right) + \underline{\hat{f}}(\underline{\tilde{x}}) = \underline{f}_e(t) \quad (16)$$

where the non-linear forces vector $\underline{\hat{f}}(t,\underline{q},\underline{\dot{q}})$ is approximated by the generalized Fourier series in a condensed form

$$\underline{\hat{f}}(t,\underline{q},\underline{\dot{q}}) = \frac{\underline{c}_0}{\sqrt{2}} + \sum_{\underline{k}\in\mathbb{Z}^p}\underline{c}_{\underline{k}}\cos\left(\underline{k}.\underline{\omega}\right)t + \sum_{\underline{k}\in\mathbb{Z}^p}\underline{d}_{\underline{k}}\sin\left(\underline{k}.\underline{\omega}\right)t \quad (17)$$

Thus, the non-linear equations (16) can be rewritten in the form of an algebraic equation system similar to (4) for unknown vector of harmonic coefficients with only terms at positive frequency combinations. In this case $\underline{\tilde{x}}$ denotes the unknown vector of harmonic coefficients $\underline{a}_0$, $\underline{a}_{\underline{k}}$ and $\underline{b}_{\underline{k}}$

$$\underline{\tilde{x}} = \left\{\begin{array}{cccccccc} \frac{\underline{a}_0^T}{\sqrt{2}} & \underline{a}_{\underline{1}}^T & \underline{b}_{\underline{1}}^T & \underline{a}_{\underline{2}}^T & \underline{b}_{\underline{2}}^T & \cdots & \underline{a}_{\underline{N}}^T & \underline{b}_{\underline{N}}^T \end{array}\right\}^T \quad (18)$$

where N represents the total number of frequency components including all harmonic terms up to m of each frequency direction and all the coupling frequencies chosen by using (11). $\underline{H_{\mathrm{e}}}$ and $\underline{\hat{H}}(\underline{\tilde{x}})$ contain the projection of the external forces $\underline{f}_e(t)$ and the non-linear part $\underline{\hat{f}}(t,\underline{q},\underline{\dot{q}})$, respectively. $\underline{\hat{H}}(\underline{\tilde{x}})$ is given by

$$\underline{\hat{H}}(\underline{\tilde{x}}) = \left\{\begin{array}{cccccccc} \frac{\underline{c}_0^T}{\sqrt{2}} & \underline{c}_{\underline{1}}^T & \underline{d}_{\underline{1}}^T & \underline{c}_{\underline{2}}^T & \underline{d}_{\underline{2}}^T & \cdots & \underline{c}_{\underline{N}}^T & \underline{d}_{\underline{N}}^T \end{array}\right\}^T \quad (19)$$

The non-linear treatment of Fourier coefficients is performed by extending the generalization of the AFT to a p-dimensional frequency domain with a p-dimensional FFT. $\underline{\underline{H_{\mathrm{l}}}}$ contains the contribution of the linear part of (1) and refers to the block diagonal matrix:

$$\underline{\underline{H_{\mathrm{l}}}} = \begin{bmatrix} \underline{\underline{K}} & \underline{\underline{0}} & \cdots & \\ \underline{\underline{0}} & \underline{\underline{\Lambda_1}} & \underline{\underline{0}} & \cdots \\ \cdots & \underline{\underline{0}} & \underline{\underline{\Lambda_k}} & \underline{\underline{0}} \\ & \cdots & \underline{\underline{0}} & \underline{\underline{\Lambda_N}} \end{bmatrix} \quad (20)$$

with

$$\underline{\underline{\Lambda_k}} = \begin{bmatrix} \underline{\underline{K}} - (\underline{k}.\underline{\omega})^2\,\underline{\underline{M}} & (\underline{k}.\underline{\omega})\,\underline{\underline{C}} \\ -(\underline{k}.\underline{\omega})\,\underline{\underline{C}} & \underline{\underline{K}} - (\underline{k}.\underline{\omega})^2\,\underline{\underline{M}} \end{bmatrix} \text{ for } k \in [1,N] \quad (21)$$

4. Condensation procedure

If the considered non-linear system has n degrees of freedom but only q of them are used in the formula of the non-linear forces $\underline{\hat{f}}(t, \underline{q}, \underline{\dot{q}})$, then it is possible to work with a system similar to (4) but with size $q(2m+1)$ instead of $n(2m+1)$. For systems with localized non-linearities, this kind of condensation is very interesting (Hahn & Chen, 1994; Sinou, 2008). To achieve this, one has to partition the variables into the p linear ones, denoted $\underline{q}^{\mathrm{l}}$, and the q non-linear ones, denoted $\underline{q}^{\mathrm{nl}}$. This implies later a partition of $\underline{\tilde{x}}$ into $\underline{\tilde{x}}^{\mathrm{l}}$ and $\underline{\tilde{x}}^{\mathrm{nl}}$, reflecting the harmonic components of linear degrees of freedom and non-linear ones respectively. A relation can then be established that let us express $\underline{\tilde{x}}^{\mathrm{l}}$ as function of $\underline{\tilde{x}}^{\mathrm{nl}}$. First, this relationship is exposed and used to get the reduced non-linear system to solve. In a second part, the link between $\underline{q}$ partition and $\underline{\tilde{x}}$ partition is detailed in order to get the expressions of the partitioned HBM elements. The procedure is exposed in the case of a simple Harmonic Balance Method but can easily be extended to the case of quasi-periodic solutions.

4.1 Working with a smaller system

Once the partition is achieved, (4) can be rewritten

$$\begin{bmatrix} \underline{\underline{H}}_{\mathrm{l}}^{\mathrm{ll}} & \underline{\underline{H}}_{\mathrm{l}}^{\mathrm{lnl}} \\ \underline{\underline{H}}_{\mathrm{l}}^{\mathrm{nll}} & \underline{\underline{H}}_{\mathrm{l}}^{\mathrm{nlnl}} \end{bmatrix} \begin{Bmatrix} \underline{\tilde{x}}^{\mathrm{l}} \\ \underline{\tilde{x}}^{\mathrm{nl}} \end{Bmatrix} + \begin{Bmatrix} \underline{\hat{H}}^{\mathrm{l}}(\underline{\tilde{x}}^{\mathrm{nl}}) \\ \underline{\hat{H}}^{\mathrm{nl}}(\underline{\tilde{x}}^{\mathrm{nl}}) \end{Bmatrix} - \begin{Bmatrix} \underline{H}_{\mathrm{e}}^{\mathrm{l}} \\ \underline{H}_{\mathrm{e}}^{\mathrm{nl}} \end{Bmatrix} = \underline{0} \tag{22}$$

The first set of lines provides a relationship between $\underline{\tilde{x}}^{\mathrm{l}}$ and $\underline{\tilde{x}}^{\mathrm{nl}}$:

$$\underline{\tilde{x}}^{\mathrm{l}} = \underline{\underline{H}}_{\mathrm{l}}^{\mathrm{ll}\,-1} \left[\underline{H}_{\mathrm{e}}^{\mathrm{l}} - \underline{\underline{H}}_{\mathrm{l}}^{\mathrm{lnl}} \underline{\tilde{x}}^{\mathrm{nl}} - \underline{\hat{H}}^{\mathrm{l}}(\underline{\tilde{x}}^{\mathrm{nl}}) \right] \tag{23}$$

This expression is used to replace $\underline{\tilde{x}}^{\mathrm{l}}$ in the second set of equations, leading to a non-linear system with size $q(2m+1)$ depending on $\underline{\tilde{x}}^{\mathrm{nl}}$ only:

$$\left[\underline{\underline{H}}_{\mathrm{l}}^{\mathrm{nlnl}} - \underline{\underline{H}}_{\mathrm{l}}^{\mathrm{nll}} \underline{\underline{H}}_{\mathrm{l}}^{\mathrm{ll}\,-1} \underline{\underline{H}}_{\mathrm{l}}^{\mathrm{lnl}} \right] \underline{\tilde{x}}^{\mathrm{nl}} + \left(\underline{\hat{H}}^{\mathrm{nl}}(\underline{\tilde{x}}^{\mathrm{nl}}) - \underline{\underline{H}}_{\mathrm{l}}^{\mathrm{nll}} \underline{\underline{H}}_{\mathrm{l}}^{\mathrm{ll}\,-1} \underline{\hat{H}}^{\mathrm{l}}(\underline{\tilde{x}}^{\mathrm{nl}}) \right) - \left(\underline{H}_{\mathrm{e}}^{\mathrm{nl}} - \underline{\underline{H}}_{\mathrm{l}}^{\mathrm{nll}} \underline{\underline{H}}_{\mathrm{l}}^{\mathrm{ll}\,-1} \underline{H}_{\mathrm{e}}^{\mathrm{l}} \right) = \underline{0} \tag{24}$$

For any solution $\underline{\tilde{x}}^{\mathrm{nl}\,*}$ of (24), $\underline{\tilde{x}}^{\mathrm{l}\,*}$ is obtained thanks to equation (23).

4.2 Getting the expressions of the partitioned elements

Let us denote $\underline{\underline{R}}$ the matrix that reorders the degrees of freedom from the partitioned ones to the initial ones:

$$\underline{q} = \underline{\underline{R}} \begin{Bmatrix} \underline{q}^{\mathrm{l}} \\ \underline{q}^{\mathrm{nl}} \end{Bmatrix} \tag{25}$$

Injecting this in (1) and pre-multiplying the equation by $\underline{\underline{R}}^T$ to reorder the equations, one can write

$$\begin{bmatrix} \underline{\underline{M}}^{\mathrm{ll}} & \underline{\underline{M}}^{\mathrm{lnl}} \\ \underline{\underline{M}}^{\mathrm{nll}} & \underline{\underline{M}}^{\mathrm{nlnl}} \end{bmatrix} \begin{Bmatrix} \ddot{\underline{q}}^{\mathrm{l}} \\ \ddot{\underline{q}}^{\mathrm{nl}} \end{Bmatrix} + \begin{bmatrix} \underline{\underline{C}}^{\mathrm{ll}} & \underline{\underline{C}}^{\mathrm{lnl}} \\ \underline{\underline{C}}^{\mathrm{nll}} & \underline{\underline{C}}^{\mathrm{nlnl}} \end{bmatrix} \begin{Bmatrix} \dot{\underline{q}}^{\mathrm{l}} \\ \dot{\underline{q}}^{\mathrm{nl}} \end{Bmatrix} + \begin{bmatrix} \underline{\underline{K}}^{\mathrm{ll}} & \underline{\underline{K}}^{\mathrm{lnl}} \\ \underline{\underline{K}}^{\mathrm{nll}} & \underline{\underline{K}}^{\mathrm{nlnl}} \end{bmatrix} \begin{Bmatrix} \underline{q}^{\mathrm{l}} \\ \underline{q}^{\mathrm{nl}} \end{Bmatrix} + \begin{Bmatrix} \underline{\hat{f}}^{\mathrm{l}}(t, \underline{q}^{\mathrm{nl}}, \dot{\underline{q}}^{\mathrm{nl}}) \\ \underline{\hat{f}}^{\mathrm{nl}}(t, \underline{q}^{\mathrm{nl}}, \dot{\underline{q}}^{\mathrm{nl}}) \end{Bmatrix} = \begin{Bmatrix} \underline{f}_e^{\mathrm{l}}(t) \\ \underline{f}_e^{\mathrm{nl}}(t) \end{Bmatrix} \tag{26}$$

Projecting this set of equations onto the basis $(1/\sqrt{2}, \cos(k\omega t), \sin(k\omega t))_{(k=1,..,m)}$, one obtains a set of equations relative to $\underline{\tilde{x}}'$ vector of unknowns while equation (4) is relative to $\underline{\tilde{x}}$ and partitioned equation (22) uses $\underline{\tilde{x}}''$:

$$\underline{\tilde{x}} = \begin{Bmatrix} \underline{a}_0 \\ \underline{a}_1^{\mathrm{l}} \\ \underline{b}_1 \\ \vdots \end{Bmatrix}, \ \underline{\tilde{x}}' = \begin{Bmatrix} \underline{a}_0^{\mathrm{l}} \\ \underline{a}_0^{\mathrm{nl}} \\ \underline{a}_1^{\mathrm{l}} \\ \underline{a}_1^{\mathrm{nl}} \\ \underline{b}_1^{\mathrm{l}} \\ \underline{b}_1^{\mathrm{nl}} \\ \vdots \end{Bmatrix} \text{ and } \underline{\tilde{x}}'' = \begin{Bmatrix} \underline{\tilde{x}}^{\mathrm{l}} \\ \underline{\tilde{x}}^{\mathrm{nl}} \end{Bmatrix} = \left\{ \begin{Bmatrix} \underline{a}_0^{\mathrm{l}} \\ \underline{a}_1^{\mathrm{l}} \\ \underline{b}_1^{\mathrm{l}} \\ \vdots \end{Bmatrix} \begin{Bmatrix} \underline{a}_0^{\mathrm{nl}} \\ \underline{a}_1^{\mathrm{nl}} \\ \underline{b}_1^{\mathrm{nl}} \\ \vdots \end{Bmatrix} \right\} \tag{27}$$

This vector is related to $\underline{\tilde{x}}$ by

$$\underline{\tilde{x}} = (\underline{\underline{I}}_{2m+1} \otimes \underline{\underline{R}})\underline{\tilde{x}}' \tag{28}$$

where $\otimes$ denotes the Kronecker product.
The last step consists in linking $\underline{\tilde{x}}'$ to the vector $\underline{\tilde{x}}''$ where all the linear unknowns harmonics are at the top and all the non-linear unknowns are at the bottom:

$$\underline{\tilde{x}}' = \left[\underline{\underline{I}}_{2m+1} \otimes \begin{bmatrix} \underline{\underline{I}}_p \\ \underline{\underline{0}}_{q,p} \end{bmatrix}, \underline{\underline{I}}_{2m+1} \otimes \begin{bmatrix} \underline{\underline{0}}_{p,q} \\ \underline{\underline{I}}_q \end{bmatrix} \right] \underline{\tilde{x}}'' \tag{29}$$

Finally, partitioned and initial harmonics vectors are linked by a matrix $\underline{\underline{T}}$ with the following expression:

$$\underline{\tilde{x}} = \underbrace{\left[\underline{\underline{I}}_{2m+1} \otimes \left(\underline{\underline{R}} \begin{bmatrix} \underline{\underline{I}}_p \\ \underline{\underline{0}}_{q,p} \end{bmatrix} \right), \underline{\underline{I}}_{2m+1} \otimes \left(\underline{\underline{R}} \begin{bmatrix} \underline{\underline{0}}_{p,q} \\ \underline{\underline{I}}_q \end{bmatrix} \right) \right]}_{\underline{\underline{T}}} \underline{\tilde{x}}'' \tag{30}$$

The partitioned elements of equation (22) are obtained from the initial elements of equation (4) using

$$\begin{bmatrix} \underline{\underline{H}}_{\mathrm{l}}^{\mathrm{ll}} & \underline{\underline{H}}_{\mathrm{l}}^{\mathrm{lnl}} \\ \underline{\underline{H}}_{\mathrm{l}}^{\mathrm{nll}} & \underline{\underline{H}}_{\mathrm{l}}^{\mathrm{nlnl}} \end{bmatrix} = \underline{\underline{T}}^{T} \underline{\underline{H}}_{\mathrm{l}} \underline{\underline{T}} \tag{31a}$$

$$\begin{Bmatrix} \underline{\hat{H}}^{\mathrm{l}}(\underline{\tilde{x}}^{\mathrm{nl}}) \\ \underline{\hat{H}}^{\mathrm{nl}}(\underline{\tilde{x}}^{\mathrm{nl}}) \end{Bmatrix} = \underline{\underline{T}}^{T} \underline{\hat{H}} \tag{31b}$$

$$\begin{Bmatrix} \underline{H}_{\mathrm{e}}^{\mathrm{l}} \\ \underline{H}_{\mathrm{e}}^{\mathrm{nl}} \end{Bmatrix} = \underline{\underline{T}}^{T} \underline{H_{\mathrm{e}}} \tag{31c}$$

5. Path following: continuation

It may be useful to track the evolution of the system behaviour as one of its parameter, μ, varies. For instance in the field of rotating machinery, the behaviour of systems is often calculated for different operational speeds of interest while all the other parameters are kept constant. Special algorithms should then be implemented for two main reasons: first, such methods let us take advantage of the fact that if two values of the parameter are close, solutions of the non-linear system have good chances to be close from one another too. Second, following the path in the $(\underline{\tilde{x}}, \mu)$ space helps to find coexisting solutions for the same μ parameter value. This case is illustrated on Fig. 1 which depicts the evolution of maximum cycle amplitude versus a continuation parameter. This curve can be obtained by studying the classical Duffing oscillator which has a cubic stiffness, μ being the excitation frequency. The resonnance peak is bent on the right: this oscillator belongs to the hardening systems. Plus, there are two points B and E - turning points - at which the path folds, creating a range where multiple solutions can coexist. Without a proper continuation scheme, one would obtain at best parts A to B and C to D by looking for solutions with a positive increment in μ or parts D to E and F to A with a negative one. The B-E part of the curve would be missed in every case. Continuation algorithms are based on two main steps applied recursively for each point: first a prediction is done based on the point(s) previously obtained, then a correction step provides the new point. Different methods exist for these two steps and are exposed in the next subsections; the third subsection is dedicated to the step length adaptation techniques which basically control the distance between two consecutive points. The last part summarizes the steps and gives a global overview of the entire procedure.
The following notations will be used throughout the current section:

- $\underline{y}^{(i)} = (\underline{\tilde{x}}^{(i)}, \mu^{(i)})$: i-th converged point;
- $\underline{y}^{(i+1,0)} = (\underline{\tilde{x}}^{(i+1,0)}, \mu^{(i+1,0)})$: prediction for $(i+1)$-th point;
- $\underline{y}^{(i+1,j)} = (\underline{\tilde{x}}^{(i+1,j)}, \mu^{(i+1,j)})$: $(i+1)$-th point after j correction steps.

Moreover, to emphasize the dependency of the equation set (4) with the parameter μ, $\underline{H}(\underline{\tilde{x}})$ will be noted $\underline{H}(\underline{\tilde{x}}, \mu)$.

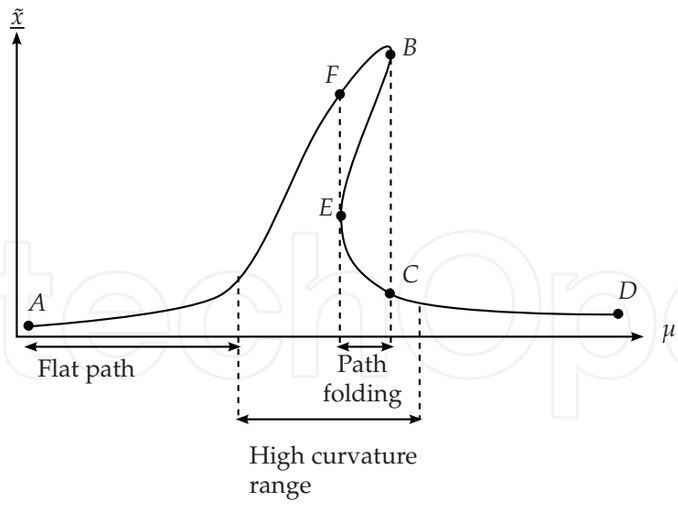

Fig. 1. Continuation applied to a typical hardening oscillator

5.1 Prediction methods

To predict a point, one needs a direction and a distance. The usual way to mesure the distance between two points is to use the following approximation of the curvilinear abscissa increment:

$$\Delta s^{(i+1)} = \sqrt{(\underline{\tilde{x}}^{(i+1)} - \underline{\tilde{x}}^{(i)})^T(\underline{\tilde{x}}^{(i+1)} - \underline{\tilde{x}}^{(i)}) + (\mu^{(i+1)} - \mu^{(i)})^2} \tag{32}$$

The way to optimize this length is discussed in subsection 5.3.
Different methods provide a direction. Among all of them one finds the secant method, the tangent method and the use of Lagrange polynomials. For most methods, one needs to have a few points already converged. To obtain these points, different values $\mu^{(i)}$, $1 \leq i \leq i_{ini}$ are chosen and usual algorithms are applied to find the corresponding solutions $\underline{\tilde{x}}^{(i)}$. The three methods exposed are illustrated on Fig. 2.

5.1.1 Secant method

The secant method (Fig. 2 (a)) uses the two previous points $(\underline{\tilde{x}}^{(i-1)}, \mu^{(i-1)})$ and $(\underline{\tilde{x}}^{(i)}, \mu^{(i)})$ to predict $(\underline{\tilde{x}}^{(i+1,0)}, \mu^{(i+1,0)})$:

$$(\underline{\tilde{x}}^{(i+1,0)}, \mu^{(i+1,0)}) = (\underline{\tilde{x}}^{(i)}, \mu^{(i)}) + \Delta s^{i+1}\left((\underline{\tilde{x}}^{(i)}, \mu^{(i)}) - (\underline{\tilde{x}}^{(i-1)}, \mu^{(i-1)})\right) \tag{33}$$

It is a very cheap predictor but it does not suit paths with small curvature radii.

5.1.2 Tangent method

This predictor (Fig. 2 (b)) uses only one previous point $(\underline{\tilde{x}}^{(i)}, \mu^{(i)})$ to predict $(\underline{\tilde{x}}^{(i+1,0)}, \mu^{(i+1,0)})$ but requires the evaluation of derivatives which can have a prohibitive cost. To evaluate the tangent vector $\overrightarrow{t} = (\overrightarrow{t_{\tilde{x}}}, t_\mu)$ to the curve at point $(\underline{\tilde{x}}^{(i)}, \mu^{(i)})$ the following steps can be used. First, get the $\overrightarrow{z}$ vector:

$$D_{\tilde{x}}\underline{H}(\underline{\tilde{x}}^{(i)}, \mu^{(i)})\overrightarrow{t_{\tilde{x}}} + D_\mu \underline{H}(\underline{\tilde{x}}^{(i)}, \mu^{(i)})t_\mu = \underline{0}$$

$$\Leftrightarrow \quad \overrightarrow{t_{\tilde{x}}} = -\underbrace{D_{\tilde{x}}\underline{H}(\underline{\tilde{x}}^{(i)},\mu^{(i)})^{-1} D_{\mu}\underline{H}(\underline{\tilde{x}}^{(i)},\mu^{(i)})}_{\overrightarrow{z}}\, t_{\mu} \tag{34}$$

where $D_{\tilde{x}}\underline{H}(\underline{\tilde{x}}^{(i)},\mu^{(i)})$ and $D_{\mu}\underline{H}(\underline{\tilde{x}}^{(i)},\mu^{(i)})$ denotes the derivatives of $\underline{H}$ with respect to $\underline{\tilde{x}}$ and μ variables respectively at point $(\underline{\tilde{x}}^{(i)},\mu^{(i)})$.
Then normalize the tangent vector:

$$\begin{aligned} & \overrightarrow{t_{\tilde{x}}}^{T}\overrightarrow{t_{\tilde{x}}} + t_{\mu}^{2} = 1 \\ \Leftrightarrow \quad & t_{\mu} = \pm 1/\sqrt{1+\overrightarrow{z}^{T}\overrightarrow{z}} \end{aligned} \tag{35}$$

The sign depends on the direction chosen to depict the curve; the positive direction is usually used. The next point can finally be predicted using

$$(\underline{\tilde{x}}^{(i+1,0)},\mu^{(i+1,0)}) = (\underline{\tilde{x}}^{(i)},\mu^{(i)}) + \Delta s^{i+1}(\overrightarrow{t_{\tilde{x}}},t_{\mu}) \tag{36}$$

5.1.3 Lagrange polynomials

This last predictor uses Lagrange polynomials of degree d to extrapolate the curve defined by the $d+1$ previous points (Fig. 2 (c)). The variable used for this polynomials is the curvilinear abscissa s. Let us redefine it locally by taking its origin at the last converged point:

$$\begin{cases} & s^{(i)} = 0, \\ \forall k \in \{1,\dots,d\}, & s^{(i-k)} = s^{(i-k+1)} - \Delta s^{(i-k+1)} \end{cases} \tag{37}$$

where $s^{(i)}$ denotes curvilinear abscissa of point $(\underline{\tilde{x}}^{(i)},\mu^{(i)})$). The Lagrange polynomials define then the unique polynomial $\mathbf{P}_d$ with degree d such that $\mathbf{P}_d(s^{(i-k)}) = \underline{y}^{(i-k)}$, $0 \le k \le d$. A classical expression of these polynomials is

$$\mathbf{P}_d(s) = \sum_{k_0=0}^{d}\left(\prod_{\substack{k=0\\k\neq k_0}}^{d}\frac{s-s^{(i-k)}}{s^{(i-k_0)}-s^{(i-k)}}\right)\underline{y}^{(i-k_0)} \tag{38}$$

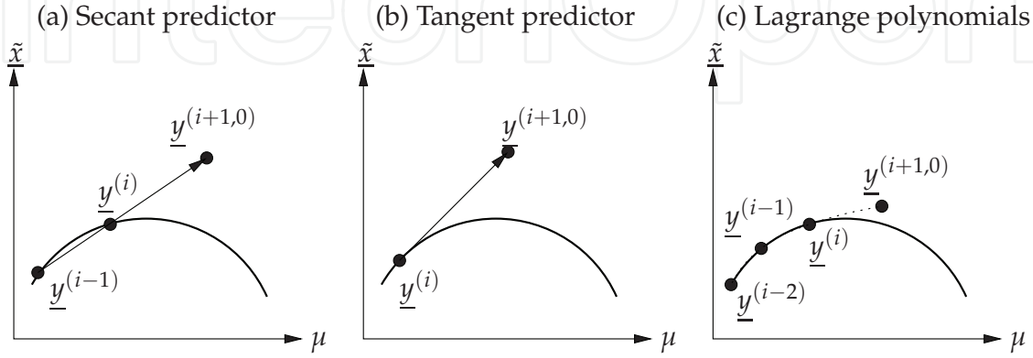

Fig. 2. Predictors illustration

The predicted point whose curvilinear abscissa is $0 + \Delta s^{(i+1)}$ is finally evaluated using

$$(\underline{\tilde{x}}^{(i+1,0)}, \mu^{(i+1,0)}) = \mathbf{P}_d(\Delta s^{(i+1)}) \tag{39}$$

Orders d greater than 2 or 3 are usually avoided because they require more operations and draw oscillating paths.

5.2 Correction methods

The aim of the correction step is to move from the predicted point that usually does not satisfy $\underline{H}(\underline{\tilde{x}}^{(i+1,0)}, \mu^{(i+1,0)}) = \underline{0}$ towards $\underline{y}^{(i+1)} = (\underline{\tilde{x}}^{(i+1)}, \mu^{(i+1)})$ that does. This is done recursively by writing

$$(\underline{\tilde{x}}^{(i+1,j+1)}, \mu^{(i+1,j+1)}) = (\underline{\tilde{x}}^{(i+1,j)} + \underline{\Delta\tilde{x}}, \mu^{(i+1,j)} + \Delta\mu) \tag{40a}$$

$$\begin{aligned} \underline{H}(\underline{\tilde{x}}^{(i+1,j+1)}, \mu^{(i+1,j+1)}) \approx \; & \underline{H}(\underline{\tilde{x}}^{(i+1,j)}, \mu^{(i+1,j)}) \\ & + D_{\tilde{x}}\underline{H}(\underline{\tilde{x}}^{(i+1,j)}, \mu^{(i+1,j)})\underline{\Delta\tilde{x}} \\ & + D_{\mu}\underline{H}(\underline{\tilde{x}}^{(i+1,j)}, \mu^{(i+1,j)})\Delta\mu \end{aligned} \tag{40b}$$

The second equation linearizes the problem around $\underline{y}^{(i+1,j)}$ to get a linear approximation that algorithms can solve to get corrections $\underline{\Delta\tilde{x}}$ and $\Delta\mu$:

$$D_{\tilde{x}}\underline{H}(\underline{\tilde{x}}^{(i+1,j)}, \mu^{(i+1,j)})\underline{\Delta\tilde{x}} + D_{\mu}\underline{H}(\underline{\tilde{x}}^{(i+1,j)}, \mu^{(i+1,j)})\Delta\mu = -\underline{H}(\underline{\tilde{x}}^{(i+1,j)}, \mu^{(i+1,j)}) \tag{41}$$

This provides $n(2m+1)$ scalar equations but there are $n(2m+1)+1$ unknowns to determine (the additional unknown being $\Delta\mu$). To get a square system, one has to add an equation. The name of the corrector depends on this equation.
Moreover, one usually limits the number of correction steps allowed to move from the predicted point towards a converged one; if this number $j_{\max}$ is reached, the correction process is aborted and a new prediction, closer to the previous one is made.

5.2.1 Constant continuation parameter

The easiest equation to add is

$$\forall j \geq 1,\ \mu^{(i+1,j)} = \mu^{(i+1,0)} \tag{42}$$

That is, the continuation parameter is kept constant and equal to the predicted value. This very simple additional constraint does not suits folding paths: using such a corrector, the path portion between the two turning points on Fig. 1 would be missed.

5.2.2 Arc length constraint

This method adds a distance condition between the corrected point and the previous converged point:

$$\forall j \geq 1,\ ||\underline{\tilde{x}}^{(i+1,j+1)} - \underline{\tilde{x}}^{(i)}||^2 + |\mu^{(i+1,j+1)} - \mu^{(i)}|^2 = (\Delta s^{(i+1)})^2 \tag{43}$$

As illustrated on Fig. 3 (a), it forces the successive point $\underline{y}^{(i+1,j)}$ to lie on the (hyper)sphere with center $\underline{y}^{(i)}$ and radius $\Delta s^{(i+1)}$.

This constraint being quadratic, it is not verified exactly and it is in fact the tangent system that is used to complete (41):

$$2\underline{\Delta\tilde{x}}^T(\underline{\tilde{x}}^{(i+1,j)} - \underline{\tilde{x}}^{(i)}) + 2\Delta\mu(\mu^{(i+1,j)} - \mu^{(i)}) = \\ (\Delta s^{(i+1)})^2 - \left(||\underline{\tilde{x}}^{(i+1,j)} - \underline{\tilde{x}}^{(i)}||^2 + |\mu^{(i+1,j)} - \mu^{(i)}|^2\right) \quad (44)$$

5.2.3 Pseudo arc length constraint

This method adds an orthogonality condition between the prediction vector $\underline{y}^{(i+1,0)} - \underline{y}^{(i)}$ and the corrected points as depicted on Fig. 3 (b):

$$\forall j \geq 1,\ (\underline{\tilde{x}}^{(i+1,0)} - \underline{\tilde{x}}^{(i+1,j+1)})^T(\underline{\tilde{x}}^{(i+1,0)} - \underline{\tilde{x}}^{(i)}) \\ + (\mu^{(i+1,0)} - \mu^{(i+1,j+1)})(\mu^{(i+1,0)} - \mu^{(i)}) = 0 \quad (45)$$

In terms of $\underline{\Delta\tilde{x}}$ and $\Delta\mu$ it gives the exact linear condition:

$$\forall j \geq 1,\ \underline{\Delta\tilde{x}}^T(\underline{\tilde{x}}^{(i+1,0)} - \underline{\tilde{x}}^{(i)}) + \Delta\mu(\mu^{(i+1,0)} - \mu^{(i)}) = 0 \quad (46)$$

5.2.4 Moore-Penrose pseudo-inverse

A last way to add a constraint is to use the Moore-Penrose pseudo-inverse matrix. This matrix provides a way to solve underconstrained systems $\underline{\underline{A}}\underline{x} = \underline{b}$ where $\underline{\underline{A}}$ has less rows than columns. The pseudo-inverse matrix of this system is

$$\underline{\underline{A^+}} = \underline{\underline{A}}^T(\underline{\underline{AA}}^T)^{-1}. \quad (47)$$

In fact, no explicit extra condition is added but it adds implicitely an orthogonality condition with the kernel of matrix $\underline{\underline{A}}$; this is illustrated in Fig. 3 (c) where $\overrightarrow{k_j}$ are representative of the kernel for the j-th correction step.
In the case of the studied system (41),

$$\underline{\underline{A}} = \left[\ D_{\tilde{x}}\underline{H}(\underline{\tilde{x}}^{(i+1,j)}, \mu^{(i+1,j)}), D_\mu\underline{H}(\underline{\tilde{x}}^{(i+1,j)}, \mu^{(i+1,j)})\ \right]. \quad (48)$$

(a) Arc length (b) Pseudo arc length (c) Moore-Penrose pseudo-inverse

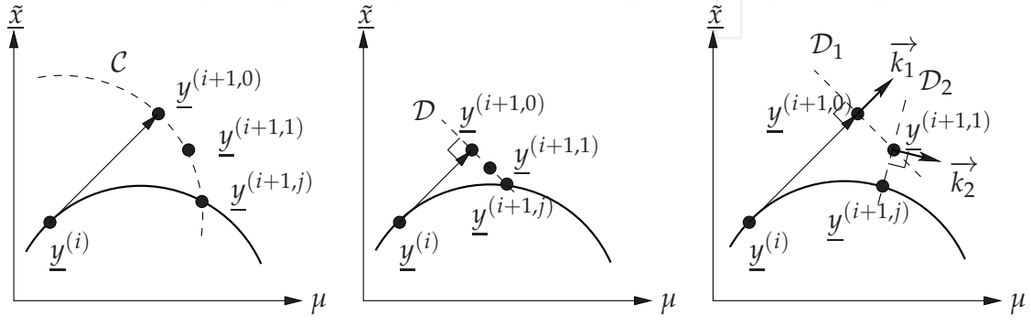

Fig. 3. Correctors illustration

5.3 Step length adaptation

As mentionned in subsection 5.1, a prediction distance has to be decided. Using a constant distance does not suit paths with regions of different curvature. Within a region of low curvature ("Flat path" on Fig. 1), the distance can be great because $\underline{\tilde{x}}$ does not vary a lot with μ; on the contrary, it is more efficient to make small steps in regions with high curvature ("High curvature range" on Fig. 1) in order to avoid a lot of correction steps.
The step length $\Delta s^{(i)}$ is adapted in two cases: if the correction procedure did not converge towards a point on the path or everytime a point is obtained. Different methods can be used to determine the step length correction (Allgower & Georg, 2003). One of the cheapest but still efficient is to monitor the number of correction steps j used to get $\underline{y}^{(i+1)}$:

- if $j = j_{\max}$, a new prediction is made with a smaller step length;
- if $j \leq j_1$, the correction process converged very quickly and $\Delta s^{(i+1)}$ can be increased;
- if $j_2 \leq j < j_{\max}$, the correction process converged slowly and a smaller step length is used for the next prediction;
- if $j_1 < j \leq j_2$, step length is left unchanged for the next prediction .

The ratios used to increase or decrease $\Delta s^{(i+1)}$ are arbitrary, as j_1, j_2 and $j_{\max}$ values. A typical set of values would be $j_1 = 2$, $j_2 = 10$, $j_{\max} = 15$ and divide $\Delta s^{(i+1)}$ by 2 to decrease it or multiply it by 2 to increase it.

5.4 Sum up

Fig. 4 summarizes the different steps of a continuation algorithm. Besides the choice of the prediction and correction methods, a few parameters have to be chosen: initial step length $\Delta s^{(1)}$, maximum number of correction iterations $j_{\max}$, as well as parameters j_1 and j_2 mentionned in section 5.3 that drive the recast of the step length. Note that the proposed convergence criterion can be slightly different. Anyhow a convergence criterion requires the choice of an ϵ value.
Finally, one needs to add a criterion for stopping the algorithm: usually a range of interest for μ is known and the algorithm is stopped as soon as a point outside this range is obtained. This is then checked each time a new point is found.

6. Conclusion

This chapter aims to provide a comprehensive overview of the basic theory of the harmonic balance methods and continuation for non-linear periodic and quasi-periodic vibrations in mechanical systems. In the past decades, these approaches have been at the focus of attention of many researchers in order to obtain very efficient tools of great importance for mechanical engineering communities. This is why, in recent years, various developments of the harmonic balance techniques have been extensively published not only to estimate the non-linear vibration of mechanical systems but also to better assess and understand some specific non-linear behaviors in mechanical systems. Moreover, the need to be able to propose more practical and commonly implemented techniques in the early stage in complex mechanical structures has led to the increase of the harmonic balance methods and new developments. Giving an exhaustive list of illustrative examples and applications showing efficiency and robustness of the harmonic balance methodology is not possible. However,

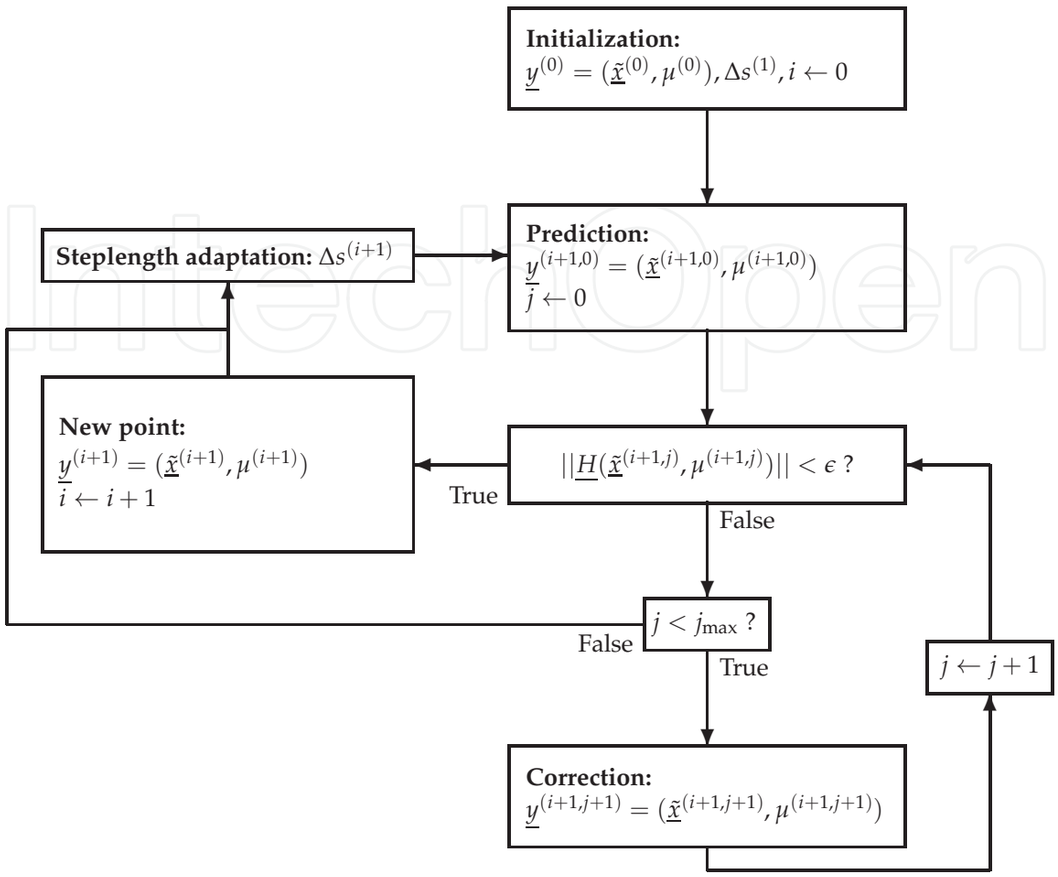

Fig. 4. General algorithm of a continuation procedure

for the interested reader, some non-exhaustive studies that have been previously published by the authors, can be found in practical cases of mechanical applications, aeronautics and car manufacturers communities, rotating machinery or structural health monitoring such as: the non-linear periodic vibration of a flexible rotor supported by ball bearings (Sinou, 2009; Villa et al., 2008), multi-dimensional harmonic balance applied to rotor dynamics (Guskov et al., 2008), the steady-state responses of autonomous mechanical systems with frictional interfaces for single or multiple input frequencies linked to unstable modes (Coudeyras, Nacivet & Sinou, 2009; Coudeyras, Sinou & Nacivet, 2009), damage detection in mechanical systems from changes in the measurement of non-linear vibrations (Sinou, 2007; 2008; Sinou & Lees, 2005; 2007), periodic non-linear response of blisks with friction ring dampers (Laxalde et al., 2007), periodic non-linear vibration for bolted structures (Jaumouillé et al., 2010), use of the Harmonic Balance Method to realize a global analysis of the dynamical behaviour of a simplified rotor supported by a squeeze-film damper (Sarrouy & Thouverez, 2010).

7. Nomenclature

$\underline{q}$	displacement vector
$\underline{\dot{q}}$	velocity vector
$\underline{\ddot{q}}$	acceleration vector
$\underline{\underline{M}}$	mass matrix
$\underline{\underline{K}}$	stiffness matrix
$\underline{\underline{C}}$	damping matrix (including gyroscopic effects if any)
$\underline{f}_e(t)$	vector of external forces
$\underline{\hat{f}}(t, \underline{q}, \underline{\dot{q}})$	vector of non-linear forces
m	order of the Fourier series
$\underline{a}_k$	Fourier coefficients of the cosine function for the k^{th} order
$\underline{b}_k$	Fourier coefficients of the sine function for the k^{th} order
$\underline{q}^{\mathrm{l}}$	p linear degrees of freedom of the system
$\underline{q}^{\mathrm{nl}}$	q non-linear degrees of freedom of the system
$\underline{\underline{A}} \otimes \underline{\underline{B}}$	Kronecker product of matrices $\underline{\underline{A}}$ and $\underline{\underline{B}}$
$D_{\tilde{x}}\underline{H}(\underline{\tilde{x}}, \mu)$	Derivatives of $\underline{H}$ function with respect to $\underline{\tilde{x}}$ at point $(\underline{\tilde{x}}, \mu)$: $\left[D_{\tilde{x}}\underline{H}(\underline{\tilde{x}}, \mu)\right]_{ij} = \frac{\partial \underline{\underline{H}}_i}{\partial \underline{\tilde{x}}_j}(\underline{\tilde{x}}, \mu)$
$D_{\mu}\underline{H}(\underline{\tilde{x}}, \mu)$	Derivatives of $\underline{H}$ function with respect to μ at point $(\underline{\tilde{x}}, \mu)$: $\left\{D_{\mu}\underline{H}(\underline{\tilde{x}}, \mu)\right\}_i = \frac{\partial \underline{\underline{H}}_i}{\partial \mu}(\underline{\tilde{x}}, \mu)$
x^T	vector or matrix transposition

8. References

Allgower, E. L. & Georg, K. (2003). *Introduction to Numerical Continuation Methods*, Springer-Verlag.

Broyden, C. G. (1965). A class of methods for solving nonlinear simultaneaous equations, *Mathematics of Computation* 19: 2024–2040.

Cameron, T. M. & Griffin, J. H. (1989). An alternating frequency/time domain method for calculating the steady-state response of nonlinear dynamic systems, *Journal of Applied Mechanics* 56(1): 149–154.

Coudeyras, N., Nacivet, S. & Sinou, J.-J. (2009). Periodic and quasi-periodic solutions for multi-instabilities involved in brake squeal, *Journal of Sound and Vibration* 328(4-5): 520–540.

Coudeyras, N., Sinou, J.-J. & Nacivet, S. (2009). A new treatment for predicting the self-excited vibrations of nonlinear systems with frictional interfaces: the constrained harmonic balance method, with application to disc brake squeal, *Journal of Sound and Vibration* 319: 1175–1199.

Guskov, M., Sinou, J.-J. & Thouverez, F. (2008). Multi-dimensional harmonic balance applied to rotor dynamics, *Mechanics Research Communications* 35: 537–545.

Hahn, E. J. & Chen, P. Y. P. (1994). Harmonic balance analysis of general squeeze film damped multidegree-of-freedom rotor bearing systems, *Journal of Tribology* 116(3): 499–507.

Jaumouillé, V., Sinou, J.-J. & Petitjean, B. (2010). An adaptive harmonic balance method for predicting the nonlinear dynamic responses of mechanical systems – application to bolted structures, *Journal of Sound and Vibration* 329(19): 4048–4067.

Kim, Y.-B. & Choi, S.-K. (1997). A multiple harmonic balance method for the internal resonant vibration of a non-linear jeffcot rotor, *Journal of Sound and Vibration* 208(3): 745–761.

Laxalde, D., Thouverez, F., Sinou, J.-J. & Lombard, J.-P. (2007). Qualitative analysis of forced response of blisks with frinction ring dampers, *European Journal of Mechanics A/Solids* 26(4): 676–687.

Sarrouy, E. & Thouverez, F. (2010). Global search of non-linear systems periodic solutions: A rotordynamics application, *Mechanical Systems and Signal Processing* 24(6): 1799–1813.

Sinou, J.-J. (2007). Effects of a crack on the stability of a non-linear rotor, *International Journal of Nonlinear Mechanics* 42(7): 959–972.

Sinou, J.-J. (2008). Detection of cracks in rotor based on the 2x and 3x super-harmonic frequency components and the crack-unbalance interactions, *Communications in Nonlinear Science and Numerical Simulation* 13(9): 2024–2040.

Sinou, J.-J. (2009). Non-linear dynamics and contacts of an unbalanced flexible rotor supported on ball bearings, *Mechanism and Machine Theory* 44(9): 1713–1732.

Sinou, J.-J. & Lees, A. (2005). Influence of cracks in rotating shafts, *Journal of Sound and Vibration* 285(4-5): 1015–1037.

Sinou, J.-J. & Lees, A. (2007). A non-linear study of a cracked rotor, *Journal of European Mechanics - A/Solids* 26(1): 152–170.

Villa, C., Sinou, J.-J. & Thouverez, F. (2008). Stability and vibration analysis of a complex flexible rotor bearing system, *Communications in Nonlinear Science and Numerical Simulation* 13(4): 804–821.

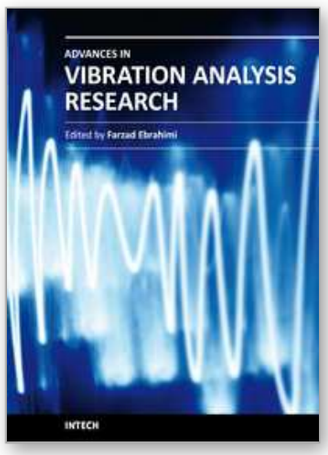

Advances in Vibration Analysis Research

Edited by Dr. Farzad Ebrahimi

ISBN 978-953-307-209-8
Hard cover, 456 pages
Publisher InTech
Published online 04, April, 2011
Published in print edition April, 2011

Vibrations are extremely important in all areas of human activities, for all sciences, technologies and industrial applications. Sometimes these Vibrations are useful but other times they are undesirable. In any case, understanding and analysis of vibrations are crucial. This book reports on the state of the art research and development findings on this very broad matter through 22 original and innovative research studies exhibiting various investigation directions. The present book is a result of contributions of experts from international scientific community working in different aspects of vibration analysis. The text is addressed not only to researchers, but also to professional engineers, students and other experts in a variety of disciplines, both academic and industrial seeking to gain a better understanding of what has been done in the field recently, and what kind of open problems are in this area.

InTech Europe
University Campus STeP Ri
Slavka Krautzeka 83/A
51000 Rijeka, Croatia
Phone: +385 (51) 770 447
Fax: +385 (51) 686 166
www.intechopen.com

InTech China
Unit 405, Office Block, Hotel Equatorial Shanghai
No.65, Yan An Road (West), Shanghai, 200040, China
中国上海市延安西路65号上海国际贵都大饭店办公楼405单元
Phone: +86-21-62489820
Fax: +86-21-62489821

IntechOpen